

Advances in High-Power Laser Diode Packaging

Teo Jin Wah Ronnie
*Singapore Institute of Manufacturing Technology,
Singapore*

1. Introduction

Rapid evolution of semiconductor laser technology and its declining cost during the last decades have made the adoption of high-power laser diodes more readily affordable. The continuous pursue for higher lasing power calls for better thermal management capability in the packaging design to facilitate controlled operation. As these laser diodes generate large amount of heat fluxes that can adversely affect their performances and reliability, a thermally-effective packaging solution is required to remove the excessive heat generated in the laser diode to its surroundings as quickly and uniformly as possible.

For high-power applications, one needs to consider not only the thermal challenges, but also the mechanical integrity of the joint as well as the electrical coupling to the remaining components in the module. These poses significant packaging challenges as these factors complicate the effort to create an ideal packaging design. Firstly, laser diodes generate large heat fluxes, up to the range of MWcm^{-2} , which causes excessive temperature rise in the active region at high injection currents. The joint which secures the laser diode onto the assembly must be able to withstand the heat generated from the laser diode and capable of maintaining its structural integrity during the long service life of the device. Secondly, the parametric performance and the reliability of these laser diodes are sensitive to both temperature and stress. During the bonding process, excessively-induced bonding stress causes the parametric performances of the laser diode to change. Furthermore, laser diode packaging requires stringent alignment tolerance in order to achieve high optical fiber coupling. On top of the aforementioned, a cost-effective packaging solution is also important because packaging usually dominates the cost of the laser diode module. Hence, the development of laser diode packaging not only is a technological challenge for achieving better performances, but also a critical step for possible commercialization of the product.

2. Thermal management of high-power laser diodes

In a laser diode package, the heat generated in the laser diode is transferred to the ambient environment by attaching a heat sink or heat spreader onto the laser diode. The laser diode must be attached to the package optimally to ensure an efficient heat transfer through the thermal interface. A thin void-free bonding interface is desired to create an effective heat dissipation channel through the die attachment process. To understand the effectiveness of its heat dissipation capability, thermal resistance calculations are usually employed to evaluate the thermal design and performance. In interface engineering, the usual measure of the heat flow in a laser diode package can be expressed as:

$$R_{package} = R_{laser\ diode} + R_{interface\ material} + R_{contact} + R_{heat\ sink} \quad (1)$$

where $R = \frac{L}{kA}$, L is the thickness, k is the thermal conductivity of the material, and A is the area of heat transfer.

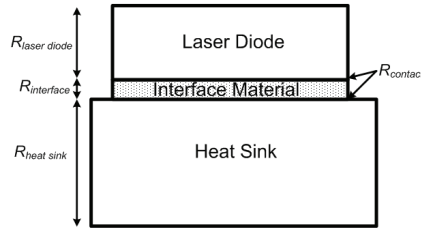


Fig. 1. Schematic diagram of the typical laser diode package and its associated thermal resistance.

Consequently, to improve the thermal design of the laser diode package, the thermal resistance should be minimized by:

- Bringing the heat source to the heat sink as close as possible,
- Making the interface as thin as possible,
- Increasing the thermal conductivity of the material,
- Providing intimate thermal contact between the laser diode and the heat sink.

For laser diode die attach, there are two bonding configurations; epi-side up and epi-side down (see Fig. 2). Eutectic die bonding processes for epi-side up bonding approaches have well been established by the semiconductor packaging industry (Qu, 2004; Larsson, 1990). The heat generated in the active region of the laser diode has to flow through the entire (GaAs/InP) substrate before reaching to the heat sink. The heat generated in the active region spreads laterally over the entire width of the laser as it flows to the heat sink, leading to a two-dimensional heat flow in the laser diode. This two-dimensional heat flow accounts for the logarithmical dependence of ridge width (Boudreau et al., 1993). Due to the low thermal conductivity of ternary alloys and multiple heterostructures (Capinski et al., 1999) of the laser diode, the heat generated in the active region cannot be dissipated onto the heat sink efficiently. Especially for single-mode ($\leq 4 \mu\text{m}$) ridge-waveguide laser diodes, the bulk of the heat generation is confined within the active region. This raises concerns as significant heat accumulation in the active region influences the spectral and spatial characteristics, with longitudinal modes broadening (Spagnolo et al., 2001). The optical output power will also be compromised since their performance characteristics are sensitive to the operating temperature of the laser diode.

As depicted in Fig. 2(b), epi-side down bonding is recommended for effective heat transfer since the proximity of the active region is only a few microns from the surface (Hayashi, 1992; Lee & Basavanahally, 1994; Katsura, 1990). The proximity of the active region to the top of the heat sink strongly influences the heat flow. Owing to the good thermal conductivity of the heat sink material, the heat produced in the active region is rapidly distributed to the heat sink. Substantial improvement can be achieved as the $R_{laser\ diode}$ is inversely proportional

to the ridge width for epi-side down bonded approach (Martin et al., 1992). The $R_{laser\ diode}$ for a epi-side down bonded laser diodes was reported to be $\sim 30\%$ smaller than that of a epi-side up bonded laser diodes.

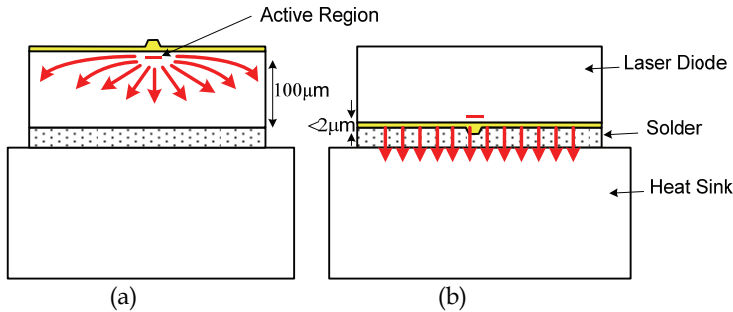


Fig. 2. Comparison of different bonding configurations of ridge-waveguide laser diodes. (a) For epi-side up bonded laser diode, the heat generated in the active region is ineffectively transferred through the substrate; (b) For epi-side down bonded laser diode, the heat flux is effectively reached the heat sink within several microns.

Epi-side down bonding also eliminates the trade-off problem between high-frequency modulation (Delpiano et al., 1994) and temperature control. In a laser diode package, three forms of electrical parasitics were present; intrinsic diode, external chip and package parasitics. For high-frequency applications, the external parasitics of the laser diode chip and the package prevent the module from achieving higher frequency modulation. In order to drive the laser diode into higher frequency modulation, epi-side down bonding approach can help to reduce the external electrical parasitics significantly. However, there are physical constraints for epi-side down bonding. The stress associated with epi-side down bonding may cause physical distortion to the device due to the mismatch in the coefficient of thermal expansion (CTE) between the laser diode and the heat sink material. As shown in Fig. 3, the laser diode will experience stresses after the die-attachment process. When the package is cooled to room temperature, the laser diode will experience compressive stresses due to the large CTE mismatch between the laser diode and the heat sink material. The close proximity between the laser diode and the heat sink further promote the strain accumulation in the active region. Relieving this stress will, hence, improve the operating life of the device (Hayakawa et al., 1983).

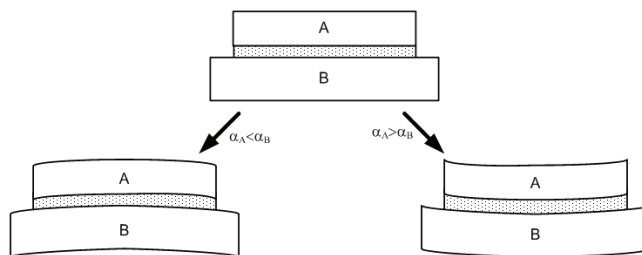


Fig. 3. Depending on the CTE properties of the two materials, compressive or tension stress can be observed after bonding.

2.1 Advanced Die-attachment techniques

After identifying that epi-side down bonding configuration as the preferred approach, the bonding process must also be able to realise the full potential of the improved thermal management capability. A major consideration in the bonding process is the formation of voids at the interface material. The primary concern with voids involves the loss of thermal conductivity. The void volumes add to the thickness to the joint volume, thus increasing the joint thickness, resulting in higher thermal resistance. Voids can cause hotspots by creating areas of poor heat dissipation paths. Voids in the thermal interface material not only limit the thermal dissipation capability but also deteriorate the electrical and mechanical properties of the joint. Continued product miniaturization and increased power density makes the importance of minimizing the void-fraction in the joint even more significant.

Hence, various die-attachment techniques have been introduced to tackle the plurality of complicating issues in epi-side down bonding approach (see Table 1). A flip-chip interconnection technique using small solder bumps (Hayashi, 1992) was introduced to resolve the alignment issues. When the solder bumps melt in the reflow process, the surface tension of the molten solder allows self-alignment and accomplishes precise chip positioning. However, thermal dissipation is compromised since heat can only be transferred through the solder bumps. Bridged die bonding (Boudreau et al., 1993) was introduced to exploit the advantage of epi-side down bonding while avoiding the stress issue by employing a solder pattern with a gap, preventing solder from having contact with the sensitive ridge. This bridged die bond geometry enhances the heat dissipation capability compared to epi-side up bonding configuration. However, this approach does not directly address the thermal issue as the heat flux generated in the active region has to be re-directed to the side of the laser diode before travelling towards the heat sink. To improve the thermal dissipation capability further, a vacuum-release process (Bascom & Bitner, 1976; Mizui & Tokuda, 1988) is recommended to produce a fluxless and virtually voidless solder bond. Epitaxial lift-off technique (Dohle et al., 1996) was also introduced to provide good bond quality between the semiconductor chip and the substrate. Ultrasonic bonding or bonding with scrubbing effect (Pittroff, 2001, 2002) was proposed to resolve any surface irregularities during bonding. However, special care must be taken as the solder material may bridge onto the facet easily, obscuring the emitted laser beam for edge-emitting laser diodes. The stress induced by the scrubbing process should be limited to avert any damage incurred on the laser diodes.

In general, $R_{interface\ material}$ can be reduced by applying a pressure to ensure good thermal contact between the laser diode and the solder material during the bonding (solder reflow) process. The pressure induces compressive stress onto the laser diode which may cause structural distortion to the device. Molten-state bonding (Tew et al., 2004) was proposed to alleviate the bonding stress induced. The solder material was pre-heated into molten state before a pressure is applied. Due to its molten state, the pressure applied onto the laser diode was minimal. At the same time, the bonding temperature can be lowered and the bonding time is reduced to mere seconds. This is potentially advantageous for high-volume production where a rapid bonding cycle is favoured. However, just like ultrasonic bonding or scrubbing approach mentioned earlier, the bonding parameters and conditions must be optimized (Teo et al., 2008).

Bonding Method	Bonding Parameters	Solder
Solder bump chip bonding (Hayashi 1990, 1992)	230 °C, 60 secs,	In-Pb
Vacuum-release process (Bascom & Bitner, 1976; Mizui & Tokuda, 1988)	133.3 Pa, 1 sec	Pb37Sn63
Composite solder structure (Lee & Wang, 1991, 1992)	320 °C, 13 mins 0.276 MPa	Au-Sn
Bridge die bonding (Boudreau et al., 1993)	230 °C, 1 min	In
Epitaxial lift-off (Dohle et al., 1996)	235 °C, 30 secs, 0.345 MPa	Au-Sn
Pulsed heated thermode (Pittroff, 2001, 2002)	370 °C, 5 secs, 0.375 MPa	Au80Sn20
Controlled solder interdiffusion (Merritt et al., 1997)	157-232 °C, 1 MPa	In-Sn
Molten-state bonding (Teo et al., 2004, 2008)	290-310 °C, few secs	Au80Sn20

Table 1. Comparison of various bonding techniques proposed for laser diode packaging. The bonding parameters depend largely on the bonding technique and interface material used.

2.2 Thermal interface materials

As shown in Table 2, solders are utilized in every part of a laser diode assembly due to their electrical interconnect, mechanical support and heat dissipation capabilities. These solders can be commonly categorized into two types; hard solder and soft solder. The decision to use soft or hard solder is based on the optimization of a number of properties, including solder strength, solder migration, creep, fatigue, whisker formation, stress, thermal expansion, liquidus temperature, and thermal conductivity of each solder type. It is also dependent on the application as well as the hierarchy of the package.

In general, the solder material must satisfy the following requirements:

- Have the desired processing temperature to support high temperature operation
- Provide sufficient wetting characteristics to form metallurgical bond between the laser diode and heat sink
- Provide an efficient heat dissipating channel to the heat sink
- Reduce thermally induced stresses arise from the mismatch of thermal expansion between the laser diode and heat sink
- Exhibit no/low deformation during its long-term operation
- Exhibit low electrical resistivity to reduce Joules heating at high injection current

Table 2 shows a list of some common solder materials used in laser diode packaging. Soft solder, commonly containing large percentage of lead, tin and indium, has very low yield strength and incurs plastic deformation under stresses. Their capability to deform plastically helps to relieve the stress developed in the bonded structure. However, this makes soft solder subject to thermal fatigue and creep rupture, causing long-term reliability problems (Solomon, 1986; Lau & Rice, 1985). They are also attributed to solder instabilities like whisker growth, void formation at the bonding part, and diffusion growth (Mizuishi et al., 1983, 1984; Sabbag & McQueen, 1975). Whiskers growth may short the electrical connection

Solder	Physical Properties				
	Melting Point (°C)	Tensile Strength (MPa)	Creep Resistance	Thermal conductivity (W/m/°C)	Electrical Resistivity (μΩ.cm)
Hermetic Sealing; Eutectic die attach - fiber location - fluxless soldering					
Au88Ge12	356E	185	Excellent	44	-
Au80Sn20	280E	276	Excellent	57	16
Opto-package assembly step soldering - non amenable to fluxless soldering					
Sn63Pb37	183E	32	Moderate	50	15
96SnAgCu	215-225	~40	High	-	Na
Fiber ferrule joining					
Indium	156	2.5	Poor	80	8.8
In97Ag3	146E	5.5	Poor	73	7.5
In52Sn48	118E	11.9	Low	34	15
Component Anchoring					
Bi58Sn42	138E	55	Moderate	19	35
Bi40Sn60	138-170	-	Moderate	21	38

Table 2. Comparison of various solder materials used in butterfly laser diode package and their physical properties [32].

and obstruct its optical beam. As mentioned earlier, the laser diode package will experience elevated temperature during operation. When the laser diode package is subjected to temperature above 65 °C, the homologous temperature of soft solder material such as Indium is more than 0.8. The solder material will experience high creep deformation, which implies a reliability concern for these solder joints. Hence, bonding of laser diodes using soft solder will face reliability problems (Shi et al., 2000, 2002). The reliability of the joint is a critical issue for the practical design and fabrication of a mechanically stable and reliable assembly.

Hard solder, on the other hand, has very high yield strength and thus incurs elastic rather than plastic deformation under stresses. Eutectic Au80Sn20 alloy are usually adopted for high-power laser diode applications to overcome the reliability issues (Fujiwara, 1982). Accordingly, it has good thermal conductivity and is free from thermal fatigue and creep movement phenomena (Matijasevic et al., 1993). Unfortunately, hard solder does not help to release the stresses developed during the bonding cycle because of low plastic deformation in the solder material.

2.3 Next generation heat sink materials

The standard heat sink material in nearly all commercially available laser diode packages is copper owing to its excellent thermal conductivity, its good mechanical machining properties, and its comparably low price. However, with the global demands for increasing output power, heat sink material with even higher thermal conductivity is desired. In response to these needs, an increasing number of ultra-high thermal conductivity materials have been and are being developed that offer significant improvements that may be suitable for high-power laser diode applications (Zweben, 2005). Not only do these materials possess very high thermal conductivity compared to traditional packaging materials, they also offer low CTE properties to reduce thermal stresses that can affect the performance and reliability of the package. While some of these materials are still at its infancy, they offer an alternative

perception of how they can contribute to future thermal management problems, especially in the area of high-power applications.

2.4 Cooling approaches for high-power applications

In most thermal management problems, removing the heat flux generated from the heat source (in this case, laser diode) to the heat sink by means of conduction alone is insufficient. To maintain its high efficiency and long lifetime, the operating temperature of the laser diode package is kept as low as possible, typically below 60 °C. Depending on the thermal power density, these heat sink materials are further cooled by means of passive- or active-cooling approaches. The design and analysis of heat sinks is one of the most extensive research areas in electronics cooling (Rodgers, 2005). The heat sinks function by extending the surface area of heat dissipating surfaces through its use of fins.

Air-cooling is traditionally associated with the use of heat sinks. The use of fan technology faces scrutiny as the acoustic noise generated and fan bearing may in some way or another affect the functionality and reliability of the application. Furthermore, the limits of air-cooling capabilities force the migration of air- to liquid or thermoelectric cooling. Liquid cooling solutions have proven to be able to manage large transient heat loads, especially in areas where design/space constraints limit the use of forced air-cooling approach. Micro-channel heat sinks are the state-of-the-art solution for maximum cooling performance (Leers, 2007, 2008). However, the integration of liquid-cooling technology raises reliability, cost and weight issues. Alternatively, thermoelectric cooler (TEC) can also be used to cool and regulate the operating temperature of the assembly. In fact, thermoelectric coolers have been widely used in a pump laser package to cool the laser diode and achieve wavelength and power stability. The TEC provide an effective negative thermal resistance to regulate the temperature in the laser diode package. Currently, TECs have very low efficiency (more commonly called coefficient of performance) and efforts to develop new TE materials with superior figure of merit (ZT) are ongoing. While each cooling approach has its advantages and limitations, the decision to employ which type of cooling approach depends largely on the thermal power density and construction of the system architecture.

2.5 Microstructure evolution of solder joint

During the bonding (solder reflow) process, a metallurgical bond is formed between the laser diode and the heat sink through the formation of intermetallic compound (IMC) at their respective interfaces. The initial formation of IMCs ensures a good thermal contact $R_{contact}$ at their interfaces. However, these IMCs continues to grow, though much more slowly, during storage and service. The growth of the interfacial IMCs depends on a number of factors, such as temperature/time, volume of solder, property of the solder alloy and the metallizations on the laser diode and heat sink. The IMC growth rate in terms of temperature and time are usually represented according to the empirical relationship,

$$X(t) = X_o + At^n \exp\left(\frac{-Q}{RT}\right) \quad (1)$$

where $X(t)$ is the layer thickness at aging time t ; X_o is the initial thickness; A is a numerical constant; Q is the apparent activation energy; T is the aging temperature, and R is the gas constant.

Continuous interfacial reaction may compromise on the integrity and reliability of the solder joint as the IMCs makes the solder joint less ductile and less capable of releasing stresses through plastic strain. Increased interfacial IMCs in the solder material also increases the thermal and electrical resistances of the bonded structure during storage and aging (Kressel, 1976; Fujiwara et al., 1979). This undesirable diffusion growth is of particular technological concern since it is always ongoing and may cause cracks and delaminations, especially in the presence of residual stress. In electronics packaging, the thickness of their solder bumps is typically several hundreds of microns while the thickness of the interfacial IMCs is a few microns. However, for laser diode die-attach, the solder joint has a thickness of only several microns. The influence of the IMC volume in the solder material will have a significant impact on the mechanical strength and reliability of the solder joint (Wong et al., 2005). In this section, three different solder materials commonly found in laser diode packaging will be reviewed.

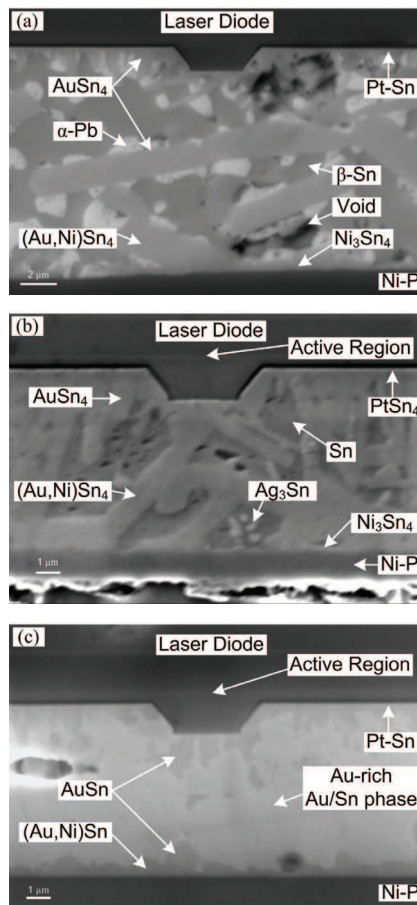


Fig. 4. Typical microstructure behaviour of as-bonded laser diode package using (a) 63Pb37Sn, (b) 3.5Ag96.5Sn, and (c) 80Au20Sn solder systems.

Fig. 4(a)-(c) shows the interfacial reaction of the as-bonded laser diode package using 63Pb37Sn, (b) 3.5Ag96.5Sn, and (c) 80Au20Sn solder systems. During reflow, PtSn and PtSn₄ IMCs were observed at the laser diode/solder interface. At the solder/heat sink interface, diffusion of Ni from the heat sink into the solder joint could be detected within 2-3 μm from the solder/heat sink interface. For both the 63Pb37Sn and 3.5Ag96.5Sn solder systems, a layer of Ni₃Sn₄ IMC was formed, followed by (Au,Ni)Sn₄ IMCs. Due to the thin solder joint, the AuSn₄ and (Au,Ni)Sn₄ IMCs could be found in the solder as well as at the interfaces. The AuSn₄ and (Au,Ni)Sn₄ IMC precipitates were randomly dispersed into the solder joint. However, for the 80Au20Sn solder system, only a thin layer of (Au,Ni)Sn IMCs was observed. The solder joint consists of three Au-Sn phases; δ (AuSn), ζ' (Au₅Sn) and β (Au₁₀Sn) phases (Teo J.W.R et al., 2008). As shown in Fig. 4(c), the δ phase was observed to coalesce to the interfaces while the Au-rich ζ' and β phases remained at the center of the solder.

During operation, the heat generated in the laser diode will caused the package to experience thermal loading. Metallurgical interaction in the solder joint will continue to occur by means of solid-state processes. Consequently, the composition, microstructure and physical properties of the solder joint changes with the device life. Fig. 5 shows the microstructure evolution of 3.5Ag96.5Sn solder joint during aging at 150 °C. Although the laser diode package may not experience such high temperature during operation, the accelerated temperature aging was often adopted to screen if the solder material and the joint is capable of meeting the desired operating lifespan of the applications.

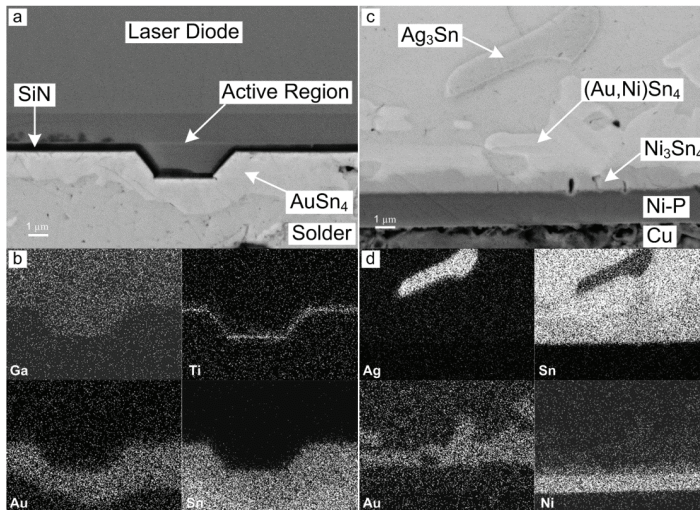


Fig. 5. Typical SEM micrographs and EDX mapping showing the development of intermetallic compound layers in a 3.5Ag96.5Sn soldered laser diode package as a result of solid-state aging at 150 °C at the (a) laser diode/solder and (c) solder/heatsink interface.

During aging, the interfacial IMC thicknesses were found to increase with aging time. For the 63Pb37Sn and 3.5Ag96.5Sn solders, the AuSn₄ and (Au,Ni)Sn₄ IMCs first settled to the interfaces and then grew with time. As depicted in Fig. 5, the (Au,Ni)Sn₄ grains separated

from the Ni(P) layer at the roots of the grains in the process of breaking off and a Ni_3Sn_4 IMC layer was formed in between the $(\text{Au,Ni})\text{Sn}_4$ IMC and the Ni(P) layer. These interfacial IMC layers, which formed a large portion of the solder joint, could grow up to a thickness of 8 μm . A thick IMC layer at the interface pose reliability concern as stress is usually concentrated around a thick IMC layer (Lee & Duh, 1999). To understand the growth kinetic, the total IMC thickness at the interfaces for the three solder systems was shown in Fig. 6. The IMC thickness for 63Pb37Sn and 3.5Ag96.5Sn solder systems was significantly large while 80Au20Sn solder joint exhibited limited Ni solubility into the solder. The IMC growth rate for 63Pb37Sn solder was initially much faster than 3.5Ag96.5Sn solder, followed by 80Au20Sn solder. When the bonded laser diodes were subjected to thermal aging at 150 °C, the homologous temperature for 63Pb37Sn, 3.5Ag96.5Sn, and 80Au20Sn solders were 0.928, 0.856, and 0.765, respectively. The diffusion activation energy for 63Pb37Sn solder was lower than 3.5Ag96.5Sn and 80Au20Sn solders. Hence, the IMC thickness for the 63Pb37Sn solder joint was initially observed to be the largest. As the aging duration increased, the IMC growth rate for the 63Pb37Sn solder joint reduced while the IMC thickness for 3.5Ag96.5Sn solder joint continued to increase. During aging, the participation of IMC formation at the interfaces reduced the overall Sn content in the solder joint. The reduced Sn composition lowered the Sn activities at the interfaces and hence, Kirkendall voids were introduced in the 63Pb37Sn solder joint. On the other hand, the main constituent of 3.5Ag96.5Sn solder is Sn. Even after 49 days of aging, the solder joint still have significant Sn content in the solder joint for further Ni-Sn and Au-Sn interdiffusion. Hence, with increased aging duration, the IMC thickness for 3.5Ag96.5Sn solder continued to grow and surpass the IMC thickness for 63Pb37Sn solder joint. It is important to restate that the interfacial IMCs such as AuSn_4 and $(\text{Au,Ni})\text{Sn}_4$ forms a large part of the R_{contact} highlighted in Eq. 1.

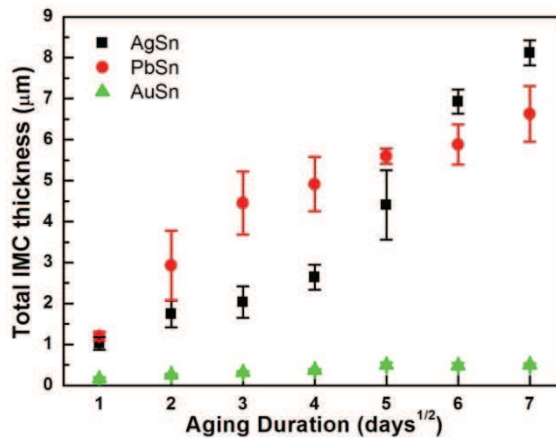


Fig. 6. Interfacial IMC growth of the three solder systems with Ni(P) metallization in solid-state reaction at 150°C.

In the 80Au20Sn system, the solder microstructure did not change significantly from the as-reflowed state (Fig. 5 (c)), even after 49 days of thermal aging. Only a thin layer of $(\text{Ni,Au})_3\text{Sn}_2$ IMC was introduced between the $\text{AuSn}(\text{Ni})$ IMC and Ni(P) layer. The slow interfacial IMC growth was due to the low Sn content in the solder joint. Furthermore,

diffusion of Sn to the interfaces was limited as the Au-rich ζ' and β phases at the center of the solder joint essentially behaved as a diffusion barrier by preventing more Sn from diffusing into the IMC layers. Hence, the introduction of $(\text{Ni,Au})_3\text{Sn}_2$ IMC rather than the growth of the $(\text{Au,Ni})\text{Sn}$ layer. The microstructure details of the three solder systems were summarized into Table 3.

Solder	Bulk	Interface (R_{contact})	
		LD	Heatsink
80Au20Sn	Au_{10}Sn (β), Au_5Sn (ζ')	Pt-Sn, AuSn	AuSn (δ), $(\text{Au,Ni})\text{Sn}$, $(\text{Ni,Au})_3\text{Sn}_2$
63Pb37Sn	α -Pb, β -Sn	Pt-Sn, AuSn_4	Ni_3Sn_4 , $(\text{Au,Ni})\text{Sn}_4$
3.5Ag96.5Sn	Sn, Ag_3Sn	Pt-Sn, AuSn_4	Ni_3Sn_4 , $(\text{Au,Ni})\text{Sn}_4$

Table 3. Microstructure summary of the three solder systems.

2.6 Structural Integrity of solder joint

Microstructure and failure mode are closely related in solder joints as the composition, microstructure and physical properties of the joint changes during aging. To assess the mechanical integrity of the solder joint, the laser diode package was subjected to shear testing, a mechanical overloading condition, to determine the weakest interface or material. Good bonding integrity with brittle fracture occurring within the laser diode was observed for all the three solder systems after bonding. The bonded laser diode exhibited a complete fracture after several microns. As shown in Fig. 7, the brittle fracture consisted of wallner lines at the GaAs material and interfacial delamination at the GaAs/SiN passivation interface of the laser diode.

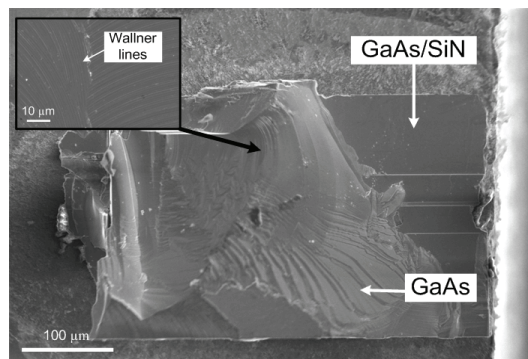


Fig. 7. Typical fracture surface examination of as-bonded LD package for the three solder systems.

During aging, the fracture mode for both 63Pb37Sn and 3.5Ag96.5Sn systems changed to ductile solder fracture as shown in Fig. 9(a)-(b). The peak shear load reduced after aging and the bonded laser diodes were completely removed after shearing off a distance of more than half the length of the laser diode (see Fig. 8). During aging, the AuSn_4 and $(\text{Au,Ni})\text{Sn}_4$ IMCs settled to the interfaces and grew. These IMCs grew into thick planar morphologies and gross defects were formed in the solder joint. These planar IMC layers reduced the

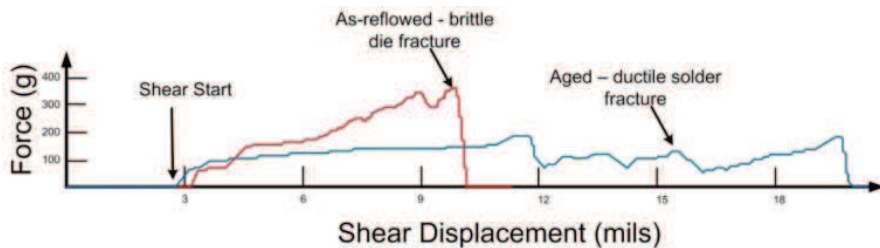


Fig. 8. Typical shear strength profile of the bonded laser diode. The mechanical strength of 63Pb37Sn and 3.5Ag96.5Sn soldered laser diode package reduced with aging.

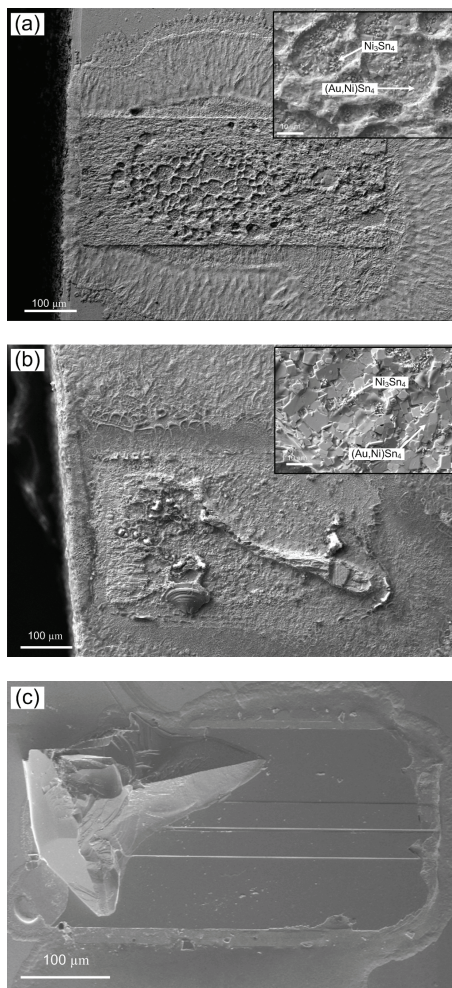


Fig. 9. Fracture surface examination of aged laser diode package for (a) 63Pb37Sn, (b) 3.5Ag96.5Sn, and (c) 80Au20Sn solder.

interfacial adhesion strength, weakening the mechanical integrity of the solder joint. This tally with the fracture surface examination that the failure mode for the aged samples has becomes more ductile. A large amount of plastic deformation was observed to occur inside the solder joint and interfacial solder/ $(\text{Au},\text{Ni})\text{Sn}_4$ and $(\text{Au},\text{Ni})\text{Sn}_4/\text{Ni}_3\text{Sn}_4$ fracture started to take place. As shown in Fig. 10, cracks were observed at the $(\text{Au},\text{Ni})\text{Sn}_4/\text{Ni}_3\text{Sn}_4$ interface. However, in the 80Au20Sn system, the failure mode did not change even after 49 days of thermal aging (see Fig. 9(c)).

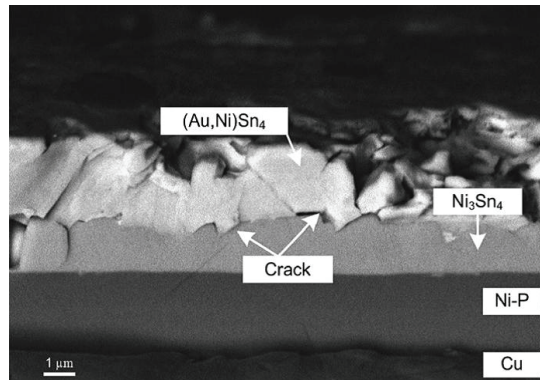


Fig. 10. Cross-sectional examination of the fracture surface at the heat sink surface after 49 days of thermal aging. The thick IMC layers have the tendency to generate structural defects.

3. Thermal behavior of laser diodes

In the previous section, we have highlighted on the importance of devising an efficient thermal management capability in the packaging design to meet the global demand for high-power applications. The heat dissipation capabilities not only depend on the selection of material and means of external cooling but also on the bonding configuration of the laser diode. Since the parametric performance of the laser diodes is strongly influenced by the heat dissipation capabilities, in this section, the thermal behaviour of the laser diodes under different bonding configurations will be evaluated and compared.

3.1 Heating response of laser diodes

Uncoated 980nm single-mode ridge-waveguide laser diodes with a cavity length of 600nm were used for this comparison study. The laser diodes were bonded onto a copper heat sink using the molten-state bonding technique (Teo et al., 2004, 2008). As shown in Fig. 11, the laser diode performance improved with higher optical power achieved after bonding. The typical power achieved for epi-side up bonded laser diodes was ~1.3 times higher whereas in epi-side down bonding approach, the optical power further improved to ~1.5 times before catastrophic damage. This shows that the lasing optical output of the laser diodes is strongly influenced by the heat dissipation capability through the die-attachment interface. Hence, understanding the heating response of the laser diodes is important to the thermal design and optimization.

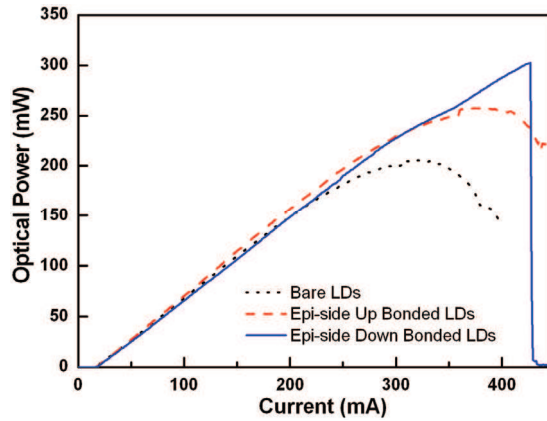


Fig. 11. Influence of bonding on the electrical-optical characteristics of the laser diode.

To understand the heat flow in the diode, it is important to study the transient behaviour of the LDs (Teo et al., 2009). Fig. 2 shows the transient heating response of the LDs at different pulse durations and duty cycles. The emission wavelength did not increase within the first 1 μs of operation. As the pulse width increased, transient heating (emission wavelength) could be observed. The temperature increased at a rate of $2.84^\circ\text{C}/\text{ms}$ and saturated within several milliseconds. Likewise, the temperature in the active region was also observed to vary with duty cycle. When the frequency of the pulse repetition rate increased above 10%, the temperature distribution across the LD was non-uniform, and the temperature in the active region increased exponentially until CW operation. At high pulse repetition rate, the temperature rise in the active region might lead to performance deterioration. From the analogy of heat conduction, the time for the excess heat energy to be transported to the GaAs substrate and reached thermal equilibrium depends on the device and its surrounding medium.

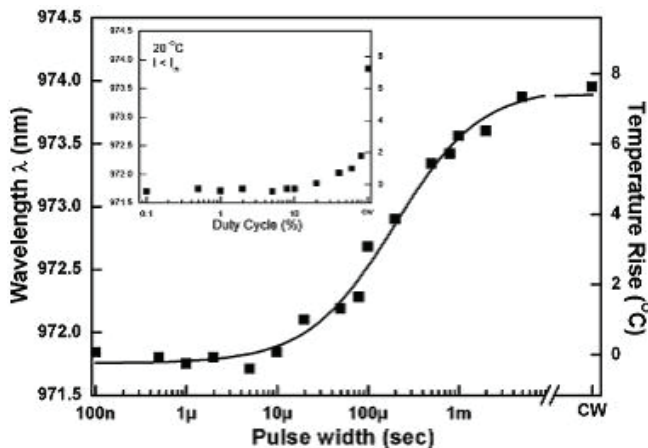


Fig. 12. Emission spectra of LDs as a function of pulse width and duty cycle. Transient heating response was observed from the spectrally resolved emission measurements.

Using Paoli method (Paoli, 1975), the temperature rise in the active region of the laser diode was estimated. Fig. 13 shows the effects of different bonding configuration on the temperature rise in the active region under pulse and continuous-wave operating conditions. In pulse operation, the temperature in the active region did not increase significantly even at a high injection current of 300 mA. This suggested that, at pulse operation, the heat sink did not have a significant influence on the thermal behaviour of the laser diodes and that the heat generated was localized within the laser diode.

However, in continuous-wave operation, Joule heating was evidently shown (see Fig. 13). For the unbonded samples, measurements were conducted until 220 mA before catastrophic damage occurred at its emitting facets. A large temperature rise of more than 100 °C could be observed in the laser diode. For epi-side up and epi-side down bonding, the heat removal means from the laser diode to the heat sink reduced the temperature in the active region at 220 mA to an average of ~70 °C and ~40 °C, respectively. Hence, higher electrical-optical measurements were permissible for epi-side up and epi-side down bonding approach. Two other characteristics were observed. First, at low injection current, the temperature rise for epi-side up bonded laser diodes and unbonded laser diodes were higher than epi-side down bonded laser diodes. The heat generated in the active region could not be removed effectively in unbonded and epi-side up bonded samples and, hence the temperature in the active region was larger than the epi-side down bonded laser diodes. Second, as the injection current increased, an exponential increment of device heating could be observed. At high injection current, additional heating source due to the series resistance of the laser diodes becomes apparent. This behaviour suggested that Joules heating was the dominant heating mechanism at high continuous-wave operating conditions.

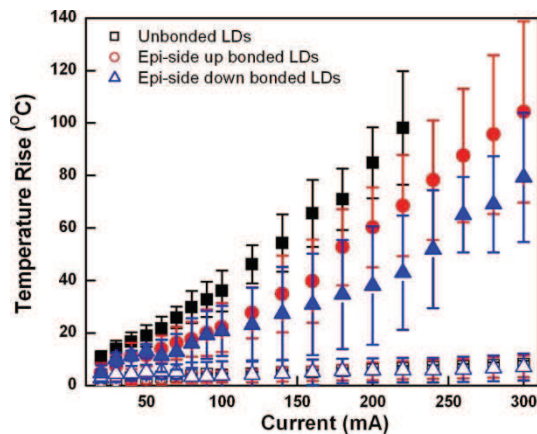


Fig. 13. Heating response of unbonded and bonded laser diodes at high pulse and continuous-wave operation. Joules heating could be observed at high continuous-wave injection current.

3.2 Thermal resistance calculation for laser diodes

Similar to interface engineering, thermal resistance calculation is a common practice to evaluate the thermal behaviour of semiconductor lasers. Typically, thermal resistance is defined as the ratio of the temperature rise in the device to the input power

$$R_{th} = \frac{\Delta T}{\Delta P} \tag{2}$$

where ΔT is the average temperature rise in the active region for a given injected power.

However, the calculation of $R_{laser\ diode}$ is not as straightforward. Equation 3 is valid only for heat generated well below the threshold current since most of the electrical input is converted into heat energy. As the current increases nearer to its threshold current, photon emission becomes more apparent (see Fig. 14). The electrical incremental input is now converted into both heat energy and coherent radiation, which can be extracted from the laser. The exponential temperature dependence of threshold current and the relative importance of Ohmic heating at high injection current further complicate in the thermal analysis as the temperature rise in the active region may not be proportional to the input power.

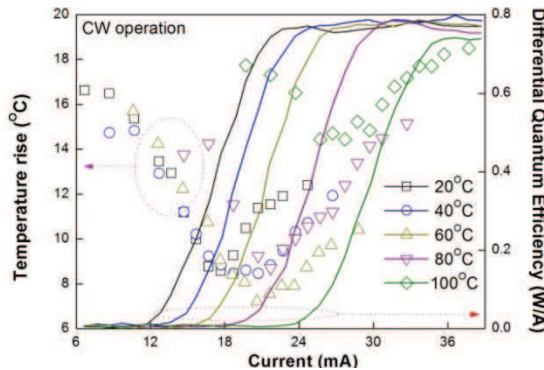


Fig. 14. Temperature rise and quantum efficiency of laser diode at different operating temperatures.

Hence, when measurements are conducted near the lasing threshold, the emitted optical power must be corrected to obtain the correct heat generation rate. Consideration of the heat generation in the active region alone is insufficient to deduce the $R_{laser\ diode}$ for high injection current. Other sources of heating element may also surface; radiative absorption of free carriers and series resistance of the diode. Firstly, the rate of photon absorption differs at different current densities. At high injection current, thermal rollover exists due to an increased of photon absorption. The heat generated in the active region is significantly large and, the effective heat generation rate for ΔP is therefore

$$\Delta P = P - \eta \cdot P = (1 - \eta)P \tag{3}$$

where η is the differential quantum efficiency of the diode. η is extracted from the LI curve. Following Eq. (2) and (3), to account for the optical absorption, the thermal resistance is change to

$$R_{laser\ diode} = \frac{\Delta T}{(1 - \eta)P} \tag{4}$$

In addition to the heat generated at the junction, Joules heating due to the series resistance R_s may also be present. At low injection current, R_s can be neglected as $IV \gg I^2R_s$. However, as the

injection current increases i.e. $IV \ll I^2R$, Joules heating becomes apparent as it increases to the square of current. Hence, the thermal resistance of the laser diode is expressed as

$$R_{laser\ diode} = \frac{\Delta T}{P + I^2R} \frac{1}{(1 - \eta)} \tag{5}$$

As shown in Fig. 15, the thermal resistance of the laser diode differs at below and above the lasing threshold. A large $R_{laser\ diode}$ of as much as 1000 °C/W could be observed below the threshold current and it dropped abruptly to 200 °C/W as it approached towards its lasing threshold value. Below the lasing threshold, the thermal resistance followed a linear regression of 130-150 °C/W per mA for all heat sink temperatures, and it remained relatively constant thereafter. The stabilized thermal resistance is terms as the ‘effective’ thermal resistance. The change of thermal resistance was induced by the transfer of non-radiative energy (non-stimulated emission) into radiative emission of free carriers as discussed earlier. This shows that the dominant cause for the temperature rise, at low injection current, is dominated by the non-radiative recombination.

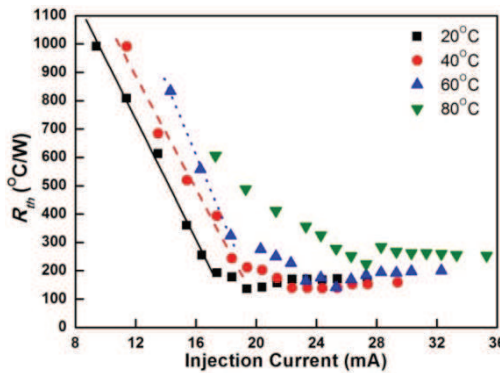


Fig. 15. Thermal resistance of laser diode at a function of current. The effective thermal resistance of the diode varies with current.

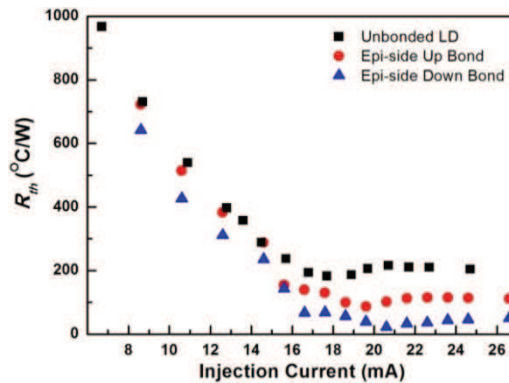


Fig. 16. Comparison of bonding configuration on the thermal resistance of laser diode package. The associated thermal resistance of the package reduced after bonding.

As shown in Fig. 16, the effective thermal resistance of the laser diode package is reduced after bonding, lowest achieved in epi-side down bonding approach. From an initial 'effective' thermal resistance of ~ 200 °C/W for the unbonded laser diodes, the 'effective' thermal resistance has now dropped to ~ 100 °C/W and ~ 40 °C/W after epi-side up and epi-side down bonding, respectively. The reduction in the thermal resistance led to improved lasing performance shown in Fig. 11.

4. Conclusion

In this chapter, the challenges in high-power laser diode packaging were identified. Material-oriented problems concerning electrical, mechanical and thermal issues must be resolved, while design-oriented issues strive for ease of manufacture, rework and inspection. The attributes of various die-attachment techniques using different kinds of interface materials to overcome the thermal management issues in the packaging design were discussed. A well-controlled void-free bonding interface is required to enable an effective heat dissipation path through the die-attachment process. The heat dissipation capabilities has a strong relationship to the parametric performance of the laser diode. Epi-side down bonding approach has lower thermal resistance, resulting in lower temperature rise in the active region and hence, permitting higher optical output power compared to epi-side up bonding approach. A preview of some of the state-of-the-art heat sink materials and various cooling methods were also discussed to expand the possibility of providing design flexibility for future demand of high-power applications.

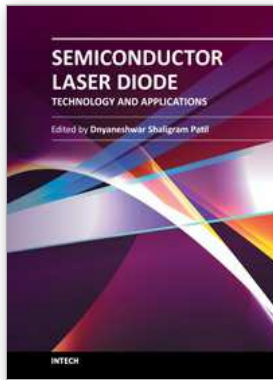
As applications continue to demand for higher optical output power and longer lifetime, thermo-mechanical stresses on the die-attachment interface pose a challenge in the laser diode package. To quantify the reliability of the laser diode package, one needs to consider not only the parametric performances of the laser diode device, but also the integrity of the joint. Knowledge on the physical changes at the interface is crucial to the understanding on the device performance and reliability. Three different solder systems - 63Pb37Sn, 3.5Ag96.5Sn and 80Au20Sn - were compared. Metallurgical bond is form between the laser diode and the heat sink through the formation of IMCs at the interfaces during bonding. For the three solder systems, the total chemical driving force arises from the dissolution of Ni from the heat sink in molten solder and from the interfacial reaction in forming IMCs. 63Pb37Sn and 3.5Ag96.5Sn solder exhibit large IMCs growth in the solder joint and the integrity of the solder joint degrades during aging. The mechanical strength of the solder joint weakens significantly and large amount of plastic deformation was observed in the solder joint during shear test. Only 80Au20Sn solder has exhibited a stable microstructure with minimal interdiffusion at the interfaces and the structural integrity of the joint was excellent. Hence, for a reliable assembly, 80Au20Sn solder is the preferred interface material to support high-power laser diode applications.

5. References

- Bascom, W. D. & Bitner J. L. (1976). *Microelectron. Reliability*, Vol. 15, No. 1, pp. 37-39, ISSN 0026-2714
- Boudreau, R.; Tabasky, M.; Armiento, C.; Bellows, A.; Cataldo, V.; Morrison, R.; Urban, M.; Sargent, R.; Negri, A. & Haugsjaa, P. (1993) Fluxless die bonding for optoelectronics, *Proceedings of 43rd Electronic Components and Technology Conference*, pp. 485 - 490, ISBN 1-4244-0985-3

- Capinski, W.S.; Maris, H.G.; Ruf, T.; Cardona, M.; Ploog, K. & Katzer, D.S. (1999) *Phys. Rev. B*, Vol. 59, No. 12, pp. 8105-8113, ISSN 1098-0121
- Delpiano, F.; Paoletti, R.; Audagnotto, P. & Puleo, M. (1994) *IEEE Trans Comp., Packag., & Manufact. Technol. B*, Vol.17, No. 3, pp. 412-417, ISSN 1070-9894
- Dohle, G.R.; Callahan, J.J.; Drabik, T.J. & Martin, K.P. (1996) A new cost effective packaging technique for optoelectronic devices *Proceedings of 46th Electronic Components and Technology Conference*, pp. 1301 – 1307, ISBN: 0-7803-3286-5
- Dohle, G.R.; Drabik, T.J.; Callahan, J.J. & Martin, K.P. (1996) *IEEE Trans. Comp., Packag., & Manufact. Technol. B*, Vol. 19, No. 3, pp. 575-580, ISSN 1070-9894
- Fujiwara, K.; Fujiwara, T.; Hori, K. & Takusagawa M. (1979) *Appl. Phys. Lett.*, Vol. 34, No. 10, pp. 668-670, ISSN 0003-6951
- Fujiwara, K.; Imai, H.; Fujiwara, T.; Hori, K. & Takusagawa M. (1979) *Appl. Phys. Lett.*, Vol. 35, No. 35, pp. 861-863, ISSN 0003-6951
- Hayakawa, T.; Miyauchi, N.; Yamamoto, S.; Hayashi, H.; Yano, S. & Hijikata T. (1983) *Appl. Phys. Lett.*, Vol. 42, No. 1, pp. 23-24, ISSN 0003-6951
- Hayashi, T. (1992). *IEEE Trans. Comp., Hybrids, & Manufact. Technol.*, Vol. 15, No. 2, pp. 225 - 230, ISSN 0148-6411
- Katsura, K.; Hayashi, T.; Ohira, F.; Hata, S.; Iwashita, K.; (1990) *J. Lightwave Technol.*, Vol. 8, No. 9, pp. 1323-1327, ISSN: 0733-8724
- Kressel, H. (1976). *Characterization of Epitaxial Semiconductor Films*, Elsevier, Amsterdam.
- Larsson, A.; Forouhar, S.; Cody, J. & Lang, R.J. (1990) *IEEE Photon. Technol. Lett.*, Vol. 2, No. 5, pp. 307-309, ISSN 1041-1135
- Lau, J. H. & Rice, D. W. (1985) *Microelectron. Reliability*, Vol. 26, No. 6, pp. 1189, ISSN 0026-2714
- Lee, C. C. & Wang, C. Y. (1992) *Thin Solid Films*, Vol. 208, No. 2, pp. 202-209, ISSN 0040-6090
- Lee, C.C.; Wang, C.Y. & Matijasevic, G.S. (1991) *IEEE Trans. Comp., Hybrids, & Manufact. Technol.*, Vol. 14, No. 2, pp. 407-412, ISSN 0148-6411
- Lee, Y. C. & Basavanahally N. (1994) *J. Minerals, Metals Mater. Society*, Vol. 46, No. 6, pp. 46-50, ISSN 1047-4838
- Lee, Y. G. & Duh J. G. (1999) *J. Materials Sci: Materials in electronics*, Vol. 10, No. 1, pp. 33-43, ISSN 0957-4522
- Leers, M.; Scholz, C.; Boucke, K. & Oudart, M. (2007). Next Generation Heat Sinks For High-Power Diode Laser Bars. *Proceedings of 23rd IEEE SEMI-THERM Symposium*, pp. 105-111, ISBN 1-4244-09589-4
- Leers, M. & Boucke, K. (2008) Cooling Approaches for High Power Diode Laser Bars. *Proceedings of 58th IEEE ECTC*, pp. 1011-1016, ISBN 978-1-4244-2230-2
- Martin, O.J.F.; Bona, G.-L. & Wolf, P. (1992) *IEEE J. Quant. Electron.*, Vol. 28, No. 11, pp. 2582-2588, ISSN 0018-9197
- Matijasevic, G. S.; Lee, C. C.; Wang C.Y. (1993). *Thin Solid Films*, Vol. 223, No. 2, pp. 276-287, ISSN 0040-6090
- Merritt, S.A.; Heim, P.J.S.; Cho, S.H.; Dagenais, M. (1997). *IEEE Trans. Comp., Packag., & Manufact. Technol. B*, Vol. 20, No.2, pp. 141-145, ISSN 1070-9894
- Mizuishi, K. (1984). *J. Appl. Phys.*, Vol. 55, No. 2, pp. 289-295, ISSN 0021-8979
- Mizuishi, K.; Sawai, M.; Todoroki, S.; Tsuji, S.; Hirao, M. & Nakamura, M. (1983) *IEEE J. Quantum Electronic*, Vol. 19, No. 8, pp. 1294-1301, ISSN 0018-9197

- Mizuishi, K. & Tokuda, M. (1988). *IEEE Trans. Comp., Hybrids, & Manufact. Technol.*, Vol. 11, No. 4, pp. 447-451, ISSN 0148-6411
- Nishiguchi, M. (1991) "Highly reliable Au-Sn eutectic bonding with background GaAs LSI chips." *IEEE Trans. Comp., Hybrids, & Manufact. Technol.* Vol. 14, No. 3, pp. 523-528, ISSN 0148-6411
- Rodgers, P.; Evely, V. & Pecht, M.G. (2005). Limits of Air-Cooling: Status and Challenges. *Proceedings of 21st IEEE SEMI-THERM Symposium*, pp. 116 – 124, ISBN 0-7803-8985-9
- Paoli, T. L. (1975) *IEEE J. Quant. Electron.* Vol. 11, No. 7, pp. 498-503, ISSN 0018-9197
- Pittroff, W.; Erbert, G.; Beister, G.; Bugge, F.; Klein, A.; Knauer, A.; Maege, J.; Ressel, P.; Sebastian, J.; Staske, R. & Traenkle, G. (2001) *IEEE Trans. Adv. Packag.* Vol. 24, No.4, pp. 434-441, ISSN 1521-3323
- Pittroff, W.; Erbert, G.; Klein, A.; Staske, R.; Sumpf, B. & Traenkle, G. (2002). Mounting of laser bars on copper heat sinks using Au/Sn solder and CuW submounts. *Proceeding of 52nd Electronic Components and Technology Conference*, pp. 276 – 281, ISBN 0-7803-7430-4
- Qu, Y.; Yuan S.; Liu, C.Y.; Bo, B.X.; Liu, G.J. & Jiang,H.L. (2004) *IEEE Photon. Technol. Lett.* Vol. 16, No. 2, pp. 389-391, ISSN 1041-1135
- Sabbag, N. A. J. & McQuuen, H. J. (1975) *Metal Finishing*, pp. 27-31
- Shi, X. Q.; Pang, H. L. J.; Wei, Z. & Wang, Z.P. (2000) *Int. J. of Fatigue*, Vol. 22, No. 3, pp. 217-228, ISSN 01421123
- Shi, X.Q.; Wang, Z.P.; Zhou, W.; Pang, H.L.J. & Yang, Q.J. (2002) *ASME J. Electron. Packag.*, Vol. 124, No. 2, pp. 85-90, ISSN 1043-7398
- Solomon, H. D. (1986) *IEEE Trans. Comp., Hybrids, & Manufact. Technol.* Vol. 9, No. 4, pp. 423-432, ISSN 0148-6411
- Spagnolo, V.; Troccoli, M.; Scamarcio, G.; Becker, C.; Glastre,G. & Sirtori, C. (2001) *Appl. Phys. Lett.* 78(9): 1177-1179, ISSN 0003-6951
- Teo, J.W.R.; Goi, L.S.K.; Xiao, L.H.; Lim, W.C.; Wang, Z.F. & Li, G.Y. (2009) *IEEE Trans. Adv. Packag.*, Vol. 32, No. 1, pp. 130-135, ISSN 1521-3323
- Teo, J.W.R.; Shi, X.Q.; Yuan, S.; Li, G.Y. & Wang, Z.F. (2008) *IEEE Trans. Comp. and Packag. Technol.*, Vol. 31, No. 2, pp. 159-167, ISSN 1521-334X
- Teo, J.W.R.; Ng, F.L.; Goi, L.S.K.; Sun, Y.F.; Wang, Z.F.; Shi, X.Q.; Wei, J. & Li, G.Y. (2008) *Microelectron. Eng.* Vol. 85, No. 3, pp. 512-517 ISSN 0167-9317
- Tew, J. W. R.; Shi, X. Q. & Shu, Y. (2004). *Materials Lett.*, Vol. 58, No. 21, pp. 2695-2699, ISSN 0167577X
- Tew, J.W.R.; Wang, Z.F.; Shi, X.Q. & Li, G.Y. (2004). An Optimized Face-Down Bonding Process for Laser Diode Packages. *Proceeding of IEEE 6th EPTC Electronics Packaging Technology Conference*, pp. 390 – 395, ISBN 0-7803-8821-6
- Wong, C.K.; Pang, J.H.L.; Sun, Y.F.; Ng, F.L.; Tew, J.W. & Fan, W.(2005) Influence of Solder Volume on Interfacial Reaction between Sn-Ag-Cu Solder and TiW/Cu/Ni UBM, *Proceeding of IEEE 7th EPTC Electronics Packaging Technology Conference*, pp. 390 – 395, ISBN 0-7803-9578-6
- Zweben, C. (2005) Ultrahigh-Thermal-Conductivity Packaging Materials, *Proceeding of 21st IEEE SEMI-THERM Symposium*, pp. 168 – 174, ISBN 0-7803-8985-9



Semiconductor Laser Diode Technology and Applications

Edited by Dr. Dnyaneshwar Shaligram Patil

ISBN 978-953-51-0549-7

Hard cover, 376 pages

Publisher InTech

Published online 25, April, 2012

Published in print edition April, 2012

This book represents a unique collection of the latest developments in the rapidly developing world of semiconductor laser diode technology and applications. An international group of distinguished contributors have covered particular aspects and the book includes optimization of semiconductor laser diode parameters for fascinating applications. This collection of chapters will be of considerable interest to engineers, scientists, technologists and physicists working in research and development in the field of semiconductor laser diode, as well as to young researchers who are at the beginning of their career.

How to reference

In order to correctly reference this scholarly work, feel free to copy and paste the following:

Teo Jin Wah Ronnie (2012). Advances in High-Power Laser Diode Packaging, Semiconductor Laser Diode Technology and Applications, Dr. Dnyaneshwar Shaligram Patil (Ed.), ISBN: 978-953-51-0549-7, InTech, Available from: <http://www.intechopen.com/books/semiconductor-laser-diode-technology-and-applications/advances-in-high-power-laser-diode-packaging>

INTECH
open science | open minds

InTech Europe

University Campus STeP Ri
Slavka Krautzeka 83/A
51000 Rijeka, Croatia
Phone: +385 (51) 770 447
Fax: +385 (51) 686 166
www.intechopen.com

InTech China

Unit 405, Office Block, Hotel Equatorial Shanghai
No.65, Yan An Road (West), Shanghai, 200040, China
中国上海市延安西路65号上海国际贵都大饭店办公楼405单元
Phone: +86-21-62489820
Fax: +86-21-62489821

© 2012 The Author(s). Licensee IntechOpen. This is an open access article distributed under the terms of the [Creative Commons Attribution 3.0 License](#), which permits unrestricted use, distribution, and reproduction in any medium, provided the original work is properly cited.